

Dielectric relaxation in a deuteron glassVarsha Banerjee^{1,*} and Sushanta Dattagupta^{2,3,†}¹*Department of Physics, Indian Institute of Technology, Hauz Khas, New Delhi-110016, India*²*S. N. Bose National Centre for Basic Sciences, J. D. Block, Salt Lake Sector III, Kolkata-700098, India*³*Jawaharlal Nehru Centre for Advanced Scientific Research, Jakkur Campus, Bangalore 560064, India*

(Received 7 January 2003; published 1 August 2003; corrected 19 August 2003)

We obtain the dielectric susceptibility of a deuteron glass based on a mean-field analysis of an Ising model with random bond strengths and random fields using a system-plus-bath approach. The two Ising pseudospin states represents two equivalent sites that the deuteron can occupy. Relaxation is caused by the random jumps of the deuteron from one site to another. It is then reasonable to assume an Arrhenius form of relaxation, on which we find that our derived results are in good qualitative agreement with experimental measurements on recently studied prototypical deuteron glasses, namely, $\text{Rb}_{1-x}(\text{ND}_4)_x\text{D}_2\text{PO}_4$ and $\text{Rb}_{1-x}(\text{ND}_4)_x\text{D}_2\text{AsO}_4$, above the glass transition.

DOI: 10.1103/PhysRevB.68.054202

PACS number(s): 75.10.Jm, 64.70.Pf, 77.22.Gm

I. INTRODUCTION

The formation of a glassy phase in mixed ferroelectric-antiferroelectric crystals continues to generate considerable experimental and theoretical interest. Among the most widely studied systems of this kind is $\text{Rb}_{1-x}(\text{ND}_4)_x\text{D}_2\text{PO}_4$, commonly denoted as D-RADP.¹⁻⁶ The Rb system by itself is ferroelectric whereas the ND_4 system by itself is antiferroelectric. The paraelectric phases of D-RDP and D-ADP are characterized by a disordered arrangement of the $\text{O-D}\cdot\cdot\text{O}$ bonds connecting the phosphate group. In D-RDP, below the ferroelectric transition temperature, the deuteron bonds order spontaneously, yielding a macroscopic electrical polarization parallel to the c axis of the crystal. In D-ADP, on the other hand, a different arrangement of the deuterons yields antiparallel dipole moments ordered perpendicularly to the c axis.

A random substitution of the ND_4 group in D-RADP breaks the ferroelectric bonds at substituted sites. For sufficient dilution, the “all up” or “all down” configurations are suppressed and the long-range order, either ferroelectric or antiferroelectric, is no longer viable. The presence of random, competing interactions makes it impossible for the deuteron bonds to satisfy all of the interactions simultaneously. Such systems are known as spin glasses. The mixed system $\text{Rb}_{1-x}(\text{ND}_4)_x\text{D}_2\text{PO}_4$ shows spin-glass behavior in the concentration range $0.22 \leq x \leq 0.8$ at low temperatures.⁷ The glassiness is a result of the freezing of $\text{O-D}\cdot\cdot\text{O}$ intrabond motion, as evidenced from experimental measurements of the dielectric permittivity.⁸ Here, because the basic random interaction is between deuterons, D-RADP is called a deuteron glass. Another widely studied deuteron glass is the deuterated rubidium ammonium arsenate $\text{Rb}_{1-x}(\text{ND}_4)_x\text{D}_2\text{AsSO}_4$ or D-RADA. Extensive experimental data on dielectric relaxation of this system exist in the literature.^{9,10}

The deuteron can occupy two sites in the $\text{O-D}\cdot\cdot\text{O}$ bond. The “left” and the “right” positions of the deuteron in the $\text{O-D}\cdot\cdot\text{O}$ bond can be mapped onto an Ising pseudospin variable σ_z which may take values $+1$ or -1 . Since the interaction between the electric dipoles is induced in the material as a result of distortion caused by the deuteron, it is long

range in character. Because of the long-range nature of the deuteron interbond coupling, the Sherrington-Kirkpatrick (SK) model for spin glasses has been adopted as the starting point for several theoretical investigations.^{11,12} However, the deuteron glass model differs from the classical spin glass in one important aspect. The random substitutional disorder ND_4 in place of Rb tilts the deuteron double well in a random fashion caused by local, random strain fields. Thus the simplest theoretical model to study deuteron glasses is the SK model with longitudinal random fields coupled linearly to the pseudospin.⁵

It is perhaps pertinent to mention here that the quantum counterpart of deuteron glass is the proton glass $\text{Rb}_{1-x}(\text{NH}_4)_x\text{H}_2\text{PO}_4$. Because hydrogen is a light quantum particle, unlike its deuterated version, the hydrogen can move among the possible two sites by a tunneling process. Tunneling can be incorporated by adding a term that couples to the transverse component of the pseudospin with respect to the easy axis of the Ising interaction. Hence the transverse Ising model with random bond strengths and random fields is the simplest possible statistical mechanical model to describe this system.¹³⁻¹⁵ On the other hand, deuterons are heavy, and therefore have extremely small tunneling frequencies. As a consequence, quantum effects are negligible in deuteron glasses. Here the deuteron is expected to jump among the possible two sites by thermal activation.

The low-frequency dielectric measurements have become an important tool to examine the relaxation time distributions and mechanisms around the glass transition temperature. In the present paper, we calculate the dielectric permittivity of a deuteron glass using a simple theoretical framework based on the mean-field approximation of the Ising model with random bonds and random fields. This model has been subjected to extensive theoretical activity in recent years. An important contribution has been made by Pirc and co-workers toward the development of the mean-field analysis of this model and the calculation of static properties.¹³ In this paper, we extend these calculations to treat relaxation effects. Our treatment is different from the recently published paper of Kim *et al.*¹⁶ in which Chamberlin *et al.*'s correlated domain model¹⁷ has been used to fit the experimental data on

the dielectric permittivity of D-RADP. On the other hand, we introduce explicit irreversible effects to study dissipative dynamics by coupling the Hamiltonian, successfully used earlier to describe the static effects,¹³ to a surrounding heat bath. Our analysis is therefore a natural extension of the corresponding static method based on an Ising model with random bonds and random fields.

The paper is organized as follows. In Sec. II, we describe the representative Hamiltonian for the deuteron glass. The mean-field analysis of the Hamiltonian is carried out in Sec. III. Section IV is devoted to the calculation of the dielectric permittivity. Finally, Sec. V contains the computed dielectric response, its analysis, and comparison with experimental observations on D-RADP and D-RADA.

II. MEAN-FIELD HAMILTONIAN

As mentioned in the Introduction, our starting Hamiltonian for the deuteron glass is thus the Ising model with long-range interactions,⁵

$$H_s = \sum_{i,j=1}^N J_{ij} \sigma_i^z \sigma_j^z - \sum_{i=1}^N f_i \sigma_i^z. \quad (1)$$

Here, J_{ij} represents the long-range interaction between the pseudospins denoting the deuteron occupation. As stated earlier, there is an additional term in H_s to incorporate the coupling between the spin and the local random field f_i representing strain fields generated by the random substitution (say, ND_4 in place of Rb). In the absence of $\{f_i\}$, the Hamiltonian of Eq. (1) is the SK model for the Ising spin glass. It is customary to assume that the distributions of J_{ij} and f_i are Gaussian and independent:

$$P(J_{ij}) = \frac{1}{\sqrt{2\pi\Delta^2}} \exp\left[-\frac{(J_{ij}-J_0)^2}{2\Delta^2}\right], \quad (2)$$

$$P(f_i) = \frac{1}{\sqrt{2\pi\Delta_f}} \exp\left[-\frac{(f_i)^2}{2\Delta_f}\right]. \quad (3)$$

Thus, Eq. (1), together with Eq. (2) and Eq. (3), describe the deuteron glass. We make a specific connection with the experimentally studied compounds^{1,2,18,19} by associating $-J$ and $+J$ coupling constants with the antiferroelectric and ferroelectric bonds and letting x and $(1-x)$ be their relative concentrations, respectively. Equating the mean and the variance of the Gaussian distribution, Eq. (2), with that of the bimodal distribution of $(\pm J)$ then requires

$$J_0 = (1-2x)J, \quad \Delta^2 = 4x(1-x)J^2. \quad (4)$$

A similar (but independent) concentration dependence can be assumed for the mean and variance of the distribution for the local random field.

We now use a mean-field approximation to replace the Hamiltonian of the interacting system by an equivalent Hamiltonian representing a noninteracting system in a self-consistent external field expressed in terms of an order parameter. A systematic mean-field theory for the deuteron

glass model represented by Eq. (1) has been carried out within replica symmetric formalism, known from the theory of spin glasses.^{8,20} Within this approach, the single-site Hamiltonian for the replica symmetric phase above the spin-glass transition temperature is written as

$$H_s = -h\sigma^z. \quad (5)$$

Here h is an effective field acting along the z axis as a result of the presence of a ‘‘ferromagnetic’’ order J_0 , the longitudinal field Δ_f , as well as a nonzero spin-glass order parameter q ,

$$h(\xi) = \frac{1}{2} \tilde{\Delta} \xi \sqrt{q + \tilde{\Delta}_f} + \tilde{J}_0 p, \quad (6)$$

$$\tilde{J}_0 = NJ_0, \quad \tilde{\Delta}_f = 4\Delta_f/J^2, \quad \tilde{\Delta} = \Delta\sqrt{N},$$

with ξ the excess static noise arising from the random interactions J_{ij} and the random fields f_i and p the local polarization.

The mean-field equations for the local polarization and the Edwards-Anderson order parameter q are

$$p(\xi) = \tanh[\beta h(\xi)], \quad (7)$$

and

$$q = \int_{-\infty}^{\infty} \frac{d\xi}{\sqrt{2\pi}} e^{-\xi^2/2} p^2(\xi). \quad (8)$$

When $J_0 = 0$, the polarization p is strictly zero at all temperatures. The spin-glass phase is characterized by a nonzero q , thus characterizing the ‘‘disordered’’ phase by both p and q being equal to zero. In deuteron and proton glasses, on the other hand, the presence of the Gaussian random field acts as an effective ordering field for the order parameter q without inducing an average polarization p . As a result, q remains finite even at temperatures much above the transition temperature under the influence of the random fields. As expected, for $\Delta_f = 0$, the above equations reduce to the corresponding equations for the SK model in the replica symmetric phase above the Almeida-Thouless line.

In disordered systems, a physically observable quantity is calculated by computing the corresponding quantity in accordance with the statistical mechanical prescription for a given realization of the disorder and then performing an averaging over the underlying probability distribution of the disorder. In proton and deuteron glasses, an additional averaging over the distribution of the random fields is essential. In the mean-field approximation the combined disorder is represented entirely in terms of the local polarization p [cf. Eq. (7)]. Thus all physical quantities are to be first calculated for a given value of p and the results averaged over the distribution of p , defined by $W(p)$. The averaged probability distribution $W(p)$ for Ising spins is defined as

$$W(p) = \frac{1}{N} \sum_i \delta(p - \langle \sigma_i^z \rangle) = \int D\xi \delta[p - p(\xi)], \quad (9)$$

where the angular brackets represent a thermal average. Equation (9) for the case $\sigma_z = \pm 1$ yields¹³

$$W(p) = \frac{1}{\beta J \sqrt{2\pi q}} \exp\left[-\frac{1}{2} \xi_0^2(p)\right] [1-p^2]^{-1}, \quad (10)$$

where $\xi_0 = \xi_0(p)$ is the inverse function of $p(\xi)$ which satisfies Eq. (7) for p in the interval $[-1, +1]$. It is easy to see that the first moment of the distribution of $W(p)$ is the total polarization (which is zero in the absence of an external electric field) while its second moment is the Edwards-Anderson order parameter q for spin glasses. With these equations at hand, which have been used earlier for calculating static properties, we now proceed to evaluate the frequency-dependent dielectric response of the deuteron glass.

III. FREQUENCY-DEPENDENT PERMITTIVITY

To study the dissipative dynamics of the spin system we have to expand the scope of the Hamiltonian in Eq. (1) by including a coupling to the surrounding bath as follows:

$$H_o = H_S + H_I + H_B. \quad (11)$$

H_I describes the interaction between the spin system and the heat bath which is characterized by the Hamiltonian H_B . As is seen later, the explicit structure of H_B does not enter our calculations of the dynamic properties. The bath, usually comprised of phonons, introduces thermal fluctuations in the spin system leading to spin “flips,” one at an instant of time. This mechanism of relaxation in an Ising model via spin-lattice coupling is referred to as the spin-flip Glauber model.²¹ Thus, the choice of H_I is dictated by the requirement that the relaxation mechanism is of the Glauber type, yielding the Boltzmann distribution at equilibrium. We assume the following type of interaction:

$$H_I = g b \sigma^x. \quad (12)$$

In Eq. (12), b is a heat-bath operator which acts on the Hilbert space of the bath Hamiltonian H_B and g is a multiplicative coupling constant. This interaction, responsible for Ising spin flips, is purely off diagonal in the representation in which H_S is diagonal. Such a coupling is known to yield Glauber kinetics for the underlying Hamiltonian,²² justifying the choice of H_I .

The dynamic susceptibility $\chi(\omega)$ evaluated within the purview of linear-response theory yields the dielectric permittivity $\epsilon(\omega)$. The two are related via the equation

$$\epsilon(\omega) = 1 + \chi(\omega). \quad (13)$$

In linear-response theory, $\chi(\omega)$ is given by²¹

$$\chi(\omega) = \beta \lim_{\delta \rightarrow 0, s \rightarrow -i\omega + \delta} [1 - s\tilde{C}(s)], \quad (14)$$

where $\tilde{C}(s)$ is the Laplace transform of the correlation function defined as

$$C(t) = \langle\langle \sigma^z(0) \sigma^z(t) \rangle\rangle. \quad (15)$$

Here the angular brackets indicate thermal as well as statistical averaging over the random bonds and fields. The quantity s is related to the applied frequency ω , δ is a small real valued parameter to ensure convergence of the Laplace transform, and β is the inverse temperature.

We now proceed to calculate the spin-correlation function of Eq. (15) which in the equilibrium ensemble is explicitly

$$C(t) = \frac{1}{Z_o} \text{Tr}[\rho_{eq} \sigma^z(0) e^{iH_o t} \sigma^z(0) e^{-iH_o t}], \quad (16)$$

where H_o is the total Hamiltonian as in Eq. (11) and Z_o is the corresponding partition function. Assuming that the coupling to the heat bath is much weaker than the thermal energy kT of the subsystem, it is possible to decompose the trace into two parts—one over the states of the subsystem and the other over the states of the heat bath. With this simplification, we can write the correlation function as²¹

$$C(t) = \frac{1}{Z_s} \text{Tr}\{e^{-\beta\tilde{H}_s} \sigma^z [U(t)]_{av} \sigma^z\}. \quad (17)$$

$[U(t)]_{av}$, referred to as the averaged time-development operator, is

$$[U(t)]_{av} = \text{Tr}_B \left(\frac{e^{-\beta H_B}}{Z_B} e^{i\mathcal{L}t} \right). \quad (18)$$

\mathcal{L} is the Liouville operator associated with the total Hamiltonian of the bath as well as the subsystem of interest. It can be decomposed as

$$\mathcal{L} = \mathcal{L}_S + \mathcal{L}_I + \mathcal{L}_B, \quad (19)$$

where \mathcal{L}_S and \mathcal{L}_B are the Liouville operators associated with the subsystem and the bath, respectively, while \mathcal{L}_I describes the interaction between the two. Since $[U(t)]_{av}$ involves a trace over the bath degrees of freedom, it therefore includes all the relaxational effects of the system.

Since dynamic measurements are in the frequency domain, it is convenient to work with the Laplace transform $[\tilde{U}(s)]_{av}$ of $[U(t)]_{av}$. Evaluation of $[\tilde{U}(s)]_{av}$ is facilitated by writing it as a resolvent expansion in which the interaction term H_I is treated perturbatively. Such an expansion yields the following general expression for the time-averaged operator:²¹

$$[\tilde{U}(s)]_{av} = [s - i\mathcal{L}_S + \tilde{\Sigma}(s)]^{-1}, \quad (20)$$

where $\tilde{\Sigma}(s)$, as specified below, contains all the information about the interactions of the heat bath and hence is aptly called the “relaxation matrix.” In order to simplify our calculations, we restrict ourselves to the Markovian approximation, which assumes that the fluctuations associated with the heat bath are characterized by frequencies which are much larger than the frequencies associated with H_S . This assumption is tantamount to ignoring certain memory effects in the system. While it is possible to evaluate $\tilde{\Sigma}(s)$ to arbitrary orders in perturbation theory, it suffices in the Markovian approximation to use an expansion up to second order in H_I , which yields

$$\tilde{\Sigma}(s) = \left(\mathcal{L}_I \frac{1}{s - i\mathcal{L}_S - i\mathcal{L}_B} \mathcal{L}_I \right)_{av}. \quad (21)$$

The correlation function can now be written explicitly as

$$\begin{aligned} \tilde{C}(s) = & \frac{1}{Z_s} \sum_{\mu, \nu, \mu', \nu'} e^{\beta h \mu} \langle \mu | \sigma^z | \nu \rangle \{ \nu \mu | [\tilde{U}(s)]_{av} | \nu' \mu' \} \\ & \times \langle \nu' | \sigma^z | \mu' \rangle. \end{aligned} \quad (22)$$

In writing this equation, we have used the properties of the Liouville operators (refer to Chap. 1 of Ref. 21) as well as the notation

$$(\mu \nu | \mathcal{L} | \mu' \nu') = \delta_{\nu \nu'} \langle \mu | H | \mu' \rangle - \delta_{\mu \mu'} \langle \nu' | H | \nu \rangle. \quad (23)$$

Using Eq. (23) the matrix elements of the superoperator \mathcal{L}_S can be written as

$$(\nu \mu | \mathcal{L}_S | \nu' \mu') = h(\mu - \nu) \delta_{\nu \nu'} \delta_{\mu \mu'}, \quad (24)$$

resulting in

$$\mathcal{L}_S = \begin{pmatrix} 0 & 0 & 0 & 0 \\ 0 & 0 & 0 & 0 \\ 0 & 0 & -2h & 0 \\ 0 & 0 & 0 & 2h \end{pmatrix}, \quad (25)$$

where the rows and columns labeled by $|\nu \mu\rangle$ take the values $|++\rangle$, $|--\rangle$, $|+-\rangle$, and $|-+\rangle$, respectively.

The Markovian approximation further allows us to write

$$\tilde{\Sigma}(s) \approx \tilde{\Sigma}(0) = \int_0^\infty dt \mathcal{L}_I e^{i(\mathcal{L}_S + \mathcal{L}_B)t} \mathcal{L}_I. \quad (26)$$

The calculation of the relaxation matrix is straightforward. A similar calculation has been done by us earlier in the context of a magnetic quantum glass, well described by the transverse Ising model.²³ In the present case, the transverse field introducing quantum effects is absent, but there is a presence of a random field at each site due to substitutional disorder. Proceeding along similar lines, we obtain from Eq. (23) and after some lengthy algebra, a typical relaxation matrix element of the following form:

$$\begin{aligned} W_{++} = & \langle ++ | \tilde{\Sigma}(0) | ++ \rangle \\ = & g^2 \int_0^{+\infty} dt [e^{+2iht} \langle b(0)b(t) \rangle + e^{-2iht} \langle b(t)b(0) \rangle]. \end{aligned} \quad (27)$$

The bath correlations are defined as

$$\langle b(t)b(0) \rangle \equiv \text{Tr} \left[\frac{e^{-\beta H_B}}{Z_B} e^{iH_B t} b(0) e^{-iH_B t} b(0) \right]. \quad (28)$$

Using the time-symmetry property of the bath correlation function, W_{++} can be rewritten as

$$W_{++} = g^2 \int_{-\infty}^{+\infty} dt e^{-2iht} \langle b(t)b(0) \rangle. \quad (29)$$

The bath correlations can be parametrized in terms of a phenomenological relaxation rate λ by making use of the following Kubo relation:

$$\int_{-\infty}^{+\infty} dt e^{+2iht} \langle b(t)b(0) \rangle = e^{2\beta h} \int_{-\infty}^{+\infty} dt e^{-2iht} \langle b(t)b(0) \rangle. \quad (30)$$

We now define λ by rewriting Eq. (30) as

$$\int_{-\infty}^{+\infty} dt e^{\pm 2iht} \langle b(t)b(0) \rangle = \lambda \frac{e^{\pm \beta h}}{e^{+\beta h} + e^{-\beta h}}, \quad (31)$$

where

$$\begin{aligned} \lambda \equiv & \int_{-\infty}^{+\infty} dt (e^{+2iht} + e^{-2iht}) \langle b(t)b(0) \rangle \\ = & \int_{-\infty}^{+\infty} dt e^{+2iht} [\langle b(t)b(0) \rangle + \langle b(0)b(t) \rangle]. \end{aligned} \quad (32)$$

Since we have restricted ourselves to the Markovian approximation, the fluctuations in the bath have a very short lifetime as compared to the time scales associated with h . Within this assumption, λ becomes real and can be approximated by the following expression:

$$\lambda \approx \int_{-\infty}^{+\infty} dt [\langle b(t)b(0) \rangle + \langle b(0)b(t) \rangle]. \quad (33)$$

Further, the Kubo relation in Eq. (30) leads to the following detailed balance conditions for transitions:

$$W_{+-} = e^{-2\beta h} W_{--} \quad (34)$$

and the Markovian approximation leads to

$$\begin{aligned} W_{++} = & -W_{+-} = \lambda p_-^{eq}, \\ W_{--} = & -W_{-+} = \lambda p_+^{eq}, \end{aligned} \quad (35)$$

where λ is given by Eq. (33) and p_\pm^{eq} denote the equilibrium probabilities

$$p_\pm^{eq} = \frac{e^{\pm \beta h}}{e^{+\beta h} + e^{-\beta h}}. \quad (36)$$

Using Eq. (25) and Eq. (35) in Eq. (26), the time-development operator can be written as

$$[U(s)]_{av} = \begin{pmatrix} 0 & 0 \\ U_A & 0 & 0 \\ 0 & 0 & U_B \\ 0 & 0 & 0 \end{pmatrix}. \quad (37)$$

Here, we have substituted

$$U_A = \frac{1}{s(s+\lambda)} \begin{pmatrix} s + \lambda p_+^{eq} & \lambda p_-^{eq} \\ \lambda p_+^{eq} & s + \lambda p_-^{eq} \end{pmatrix}, \quad (38)$$

and

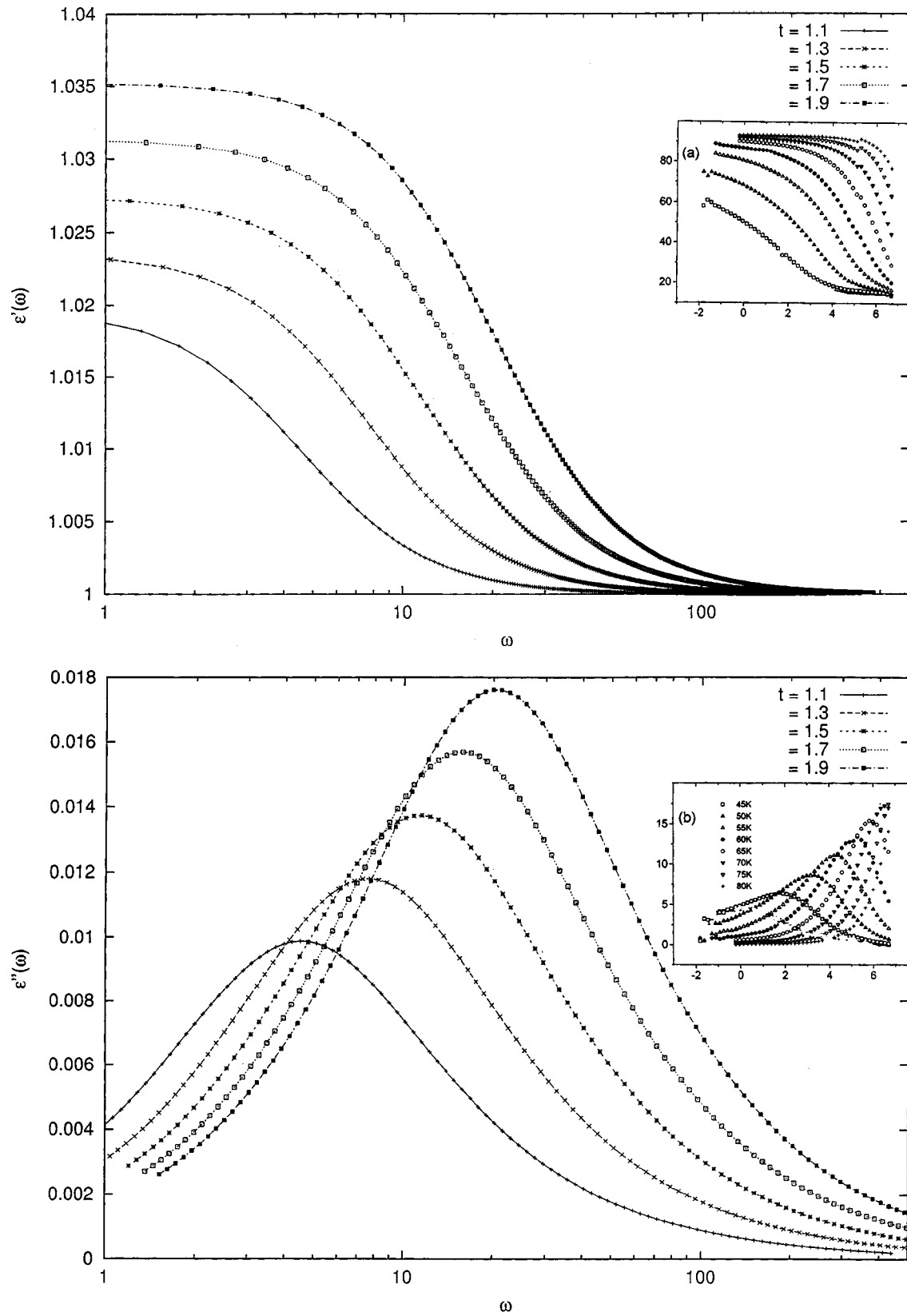


FIG. 1. Real and imaginary parts of the dielectric permittivity for a series of temperature values above the freezing temperature in (a) and (b), respectively. The insets show corresponding experimental data on D-RADP taken from Ref. 6 for qualitative comparison.

$$U_B = \frac{1}{s(s+\lambda)+4h^2} \begin{pmatrix} s+\lambda-2ih & \lambda \\ \lambda & s+\lambda+2ih \end{pmatrix}. \quad (39)$$

Inserting Eq. (37) in Eq. (22), we finally obtain the expression for the ac susceptibility as defined by Eq. (14) to be

$$\chi(\omega, p) = \beta \frac{\lambda}{\lambda - i\omega} (1 - p^2). \quad (40)$$

The local polarization p is defined by Eq. (7) as well as the relation

$$p = p_+^{eq} - p_-^{eq}. \quad (41)$$

The ac permittivity $\epsilon(\omega)$ is now easy to evaluate. Explicitly,

$$\epsilon(\omega) = 1 + \frac{1}{4\pi} \int_{-1}^1 dp W(p) \chi(\omega, p), \quad (42)$$

where $W(p)$ is as given by Eq. (9). We are now set to compute the real and imaginary parts of the dielectric permittivity and discuss the effects of temperature on these evaluations.

IV. COMPUTED DIELECTRIC PERMITTIVITY AND DISCUSSION

There are a large number of parameters in the model that are required to be fixed. In the experiments of Kim *et al.* on D-RADP, the value of x , the dilution content, was fixed at 0.4. All our evaluations are for this experimentally relevant value of x . Further, $\bar{\Delta}$ and $\bar{\Delta}_f$ have been selected on the basis of NMR and dielectric measurements to be 119.6 K and 0.34 K, respectively.⁸

Having fixed the parameters as in the above the only fitting parameter is the relaxation rate λ , related to the bath correlations, which is a function of the temperature of the bath. In the simplest model λ is assumed to follow an Arrhenius law. This form has been frequently used to obtain the distribution of relaxation times using phenomenological theories^{24,25} and is given by

$$\lambda = \lambda_o e^{-\beta \Delta E}, \quad (43)$$

where λ_o is related to the time between two consecutive attempts to pass the barrier. Although there is a report in literature that ΔE , the height of the energy barrier, increases strongly with the concentration x ,²⁴ we have selected ΔE to be 100 K. However, we have checked that the numerical computation of $\epsilon(\omega)$ is qualitatively unaffected over a range of values of ΔE .

A remark about the chosen form of the relaxation rate λ in Eq. (43) is in order. While the exponential temperature dependence is indeed what is expected for classical phonon-induced hopping over a thermal barrier, it turns out that an Arrhenius-like form ensues even when the underlying process involves tunneling but tunneling is strongly incoherent.²⁶ In that case ΔE is referred to as the ‘‘coincidence energy.’’ Such a picture of incoherent tunneling

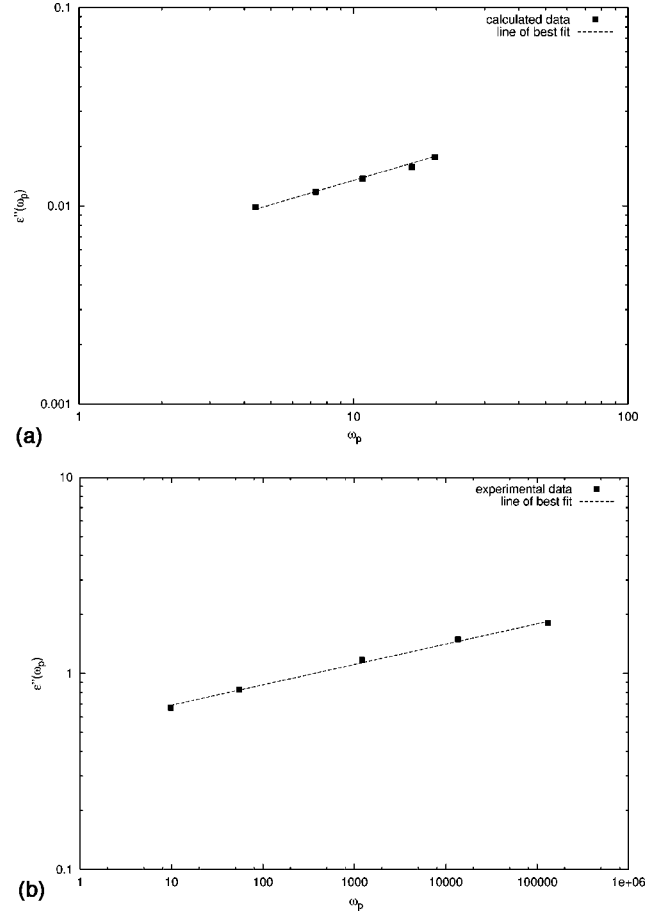


FIG. 2. Plots of peak value of $\epsilon''(\omega_p)$ versus ω_p of our theoretically obtained data (a) and corresponding experimental values from Ref. 6 (b) for different values of temperatures.

is routinely employed for describing the motion of the protons in solids.²⁷ Since deuterons are heavier than protons and are consequently endowed with smaller tunneling frequencies, it is not unexpected that even if the deuteron motion is governed by tunneling, the latter will be largely incoherent.

The results, all in units of temperature, have been obtained for $T/T_c = 1.1$ to 1.9 in steps of 0.2. T_c has been selected to be 40 K to be consistent with the experimentally studied deuteron glasses D-RADP (Ref. 6) and D-RADA.¹⁰ With this choice of temperature range, we have ensured that our evaluations are in the regime of experimental measurements, namely, just above the spin-glass phase.

In Figs. 1(a) and 1(b), we plot the real part $\epsilon'(\omega)$ and the imaginary part $\epsilon''(\omega)$ of the dielectric permittivity as a function of the frequency ω for different temperatures. Since T is lowered, they provide clear evidence that $\epsilon''(\omega)$ versus $\log \omega$ becomes more asymmetric and polydispersive. The peak becomes broader as the freezing temperature is approached. There is a shift in the peak frequency as the temperature is lowered. Further, there is also a quenching of the response at lower temperatures as envisaged by the decrease in the peak value of $\epsilon''(\omega)$. These features are quite typical of conventional spin glasses. The data exhibit qualitative

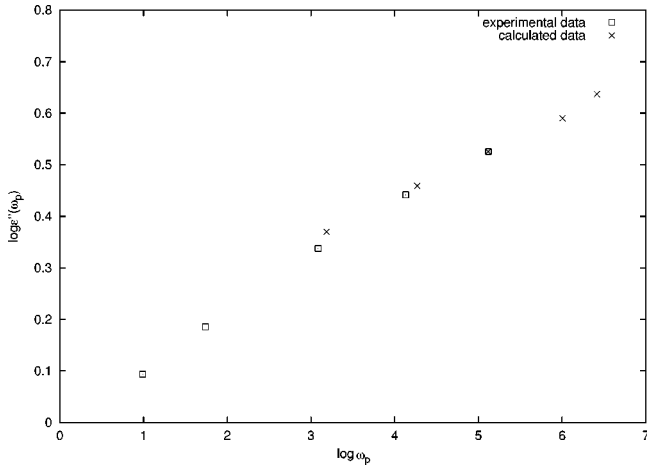


FIG. 3. Plots of $\epsilon''(\omega_p)$ versus ω_p of our scaled theoretically obtained data and corresponding experimental values from Ref. 6 for different values of temperatures.

similarities with experimental data of Kim *et al.* shown in the inset of each of the figures as regards the features mentioned above.

We point out here that the mean-field Eqs. (6)–(8) for the local field, the local polarization, and the Edwards-Anderson order parameter, respectively, have been derived within the replica symmetric formalism of the SK model. The replica symmetric solutions, which are the only stable solutions of the model, represent the high-temperature paramagnetic phase above the Almeida-Thouless line. As a consequence, the dielectric response very close to the transition temperature is expected to differ from our theoretical calculations.

In order to facilitate further qualitative comparisons of our theoretically obtained data with experimental data, we plot the peak value of $\epsilon''(\omega_p)$ versus ω_p on a double logarithmic scale in Fig. 2. Our calculated data are plotted in Fig. 2(a) while the experimental data from Ref. 6 are plotted in Fig. 2(b). Both sets of data can be fitted to straight-line equations implying a power-law dependence of $\epsilon''(\omega_p)$ on ω_p as the temperature is varied. The equations of the best-fit curves governing the two data sets are

$$Y = 0.3755X - 0.3878 \quad (\text{calculated data}), \quad (44)$$

$$Y = 0.1052 - 0.5254 \quad (\text{experimental data}), \quad (45)$$

where X and Y have been substituted for $\log(\omega_p)$ and $\log[\epsilon''(\omega_p)]$, respectively. We now try to obtain scaling factors for the X and Y coordinates of the calculated data to ensure that the two sets of data lie in the same parameter range. To achieve this, we match the values of X and Y for the point corresponding to $T=60$ K in both data sets. With this exercise, we obtain the scale factors for the X and Y coordinates for the theoretical data. The scaled data, along with the experimental data, are plotted in Fig. 3.

In Fig. 4, we plot $\epsilon''(\omega_p)$ versus T , the temperature for our calculated data (filled squares), as well as the corre-

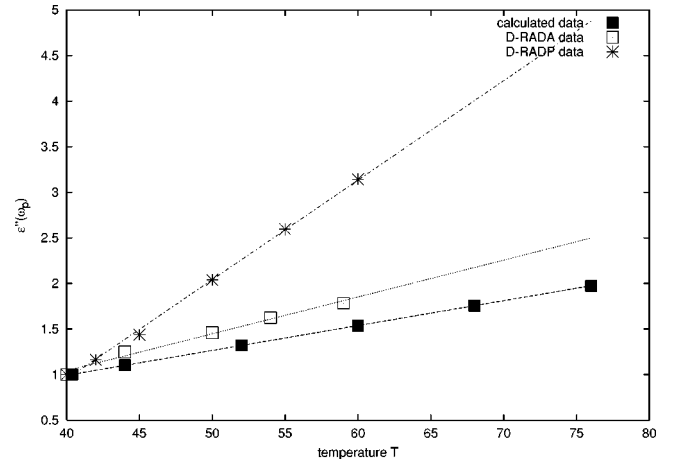


FIG. 4. Plots of $\epsilon''(\omega_p)$ versus temperature for calculated data as well as corresponding experimental data on D-RADP from Ref. 6 and on D-RADA of Ref. 10.

sponding experimental data on D-RADP (asterisks) (Ref. 6) and D-RADA (open squares) (Ref. 10). All three sets of data can be fitted to straight lines whose equations are

$$\begin{aligned} \epsilon''(\omega_p) &= 0.027T - 0.10 \quad (\text{calculated data}) \\ &= 0.04T - 0.57 \quad (\text{D-RADA data}) \\ &= 0.11T - 3.411 \quad (\text{D-RADP data}). \end{aligned}$$

These results, along with Fig. 2(c), lend credence to the approximations made in the model as well as the assumed Arrhenius relaxation in deuteron glass.

In conclusion, we may point out that analytic techniques for studying nonequilibrium phenomena are few and complicated as well. Our aim was to construct a simple model, which captures the essential ingredients of the deuteron glass but at the same time, remains analytically tractable for studying nonequilibrium properties. Because of the long-range nature of the interactions, mean-field theory is quite appropriate to calculate the static as well as the dynamic properties encapsulated by the dielectric response. Fortunately for us, the deuteron glass has well-studied experimental realizations *vis-à-vis* the D-RADP and the D-RADA systems, which have made it possible to compare our calculated data with the experimental ones to check the validity of our approximations. The mean-field calculation and our choice of the Arrhenius form for the phenomenological relaxational parameter λ yield satisfactory comparisons with experimental data.

We should also emphasize that our treatment is quite different from Chamberlin's correlated domain model¹⁷ that has been recently employed for analyzing the experimental data.^{10,16} It has been speculated that the physical origin of correlated domains in deuteron and proton glasses may be due to the quenched random fields which are of paramount importance in these systems. However, further research will be necessary in order to clarify the very existence of independently relaxing domainlike regions in deuteron glasses such as D-RADP and D-RADA. On the other hand, through-

out our analysis, we have remained faithfully close to the time-tested static approach^{4,5} and have built in the dynamical treatment as a logical extension of the static one, via heat-bath-induced relaxation phenomena.

ACKNOWLEDGMENTS

We are grateful to J. J. Kim for his experimental data on D-RADP and also for useful discussions. Support of C.S.I.R. Grant No. 03(0929)/01/EMR-II is thankfully acknowledged.

*Email address: varsha@physics.iitd.ernet.in

†Email address: sdgupta@bose.res.in

¹E. Courtens, Phys. Rev. B **33**, 2975 (1986).

²H.J. Brükner, E. Courtens, and H.-G. Unruh, Z. Phys. B: Condens. Matter **73**, 337 (1988).

³U.T. Höchli, Phys. Rev. Lett. **48**, 1494 (1982).

⁴Z. Kutnjak, C. Filipič, A. Levstik, and R. Pirc, Phys. Rev. Lett. **70**, 4015 (1993).

⁵Z. Kutnjak, R. Pirc, A. Levstik, I. Levstik, C. Filipič, R. Blinc, and R. Kind, Phys. Rev. B **50**, 12 421 (1994).

⁶Bog-Gi Kim and Jong-Jean Kim, Phys. Rev. B **55**, 5558 (1997).

⁷R. Blinc, J. Dolišek, R. Pirc, B. Tadić, and B. Zalar, Phys. Rev. Lett. **63**, 2248 (1989).

⁸A. Levstik, C. Filipič, Z. Kutnjak, I. Levstik, R. Pirc, B. Tadić, and R. Blinc, Phys. Rev. Lett. **66**, 2368 (1991).

⁹K.H. Noh, S.-I. Kwun, and J.-G. Yoon, J. Korean Phys. Soc. **32**, S824 (1998).

¹⁰K.H. Noh, S.-I. Kwun, J.-G. Yoon, and W. Kleemann, Phys. Rev. B **58**, 5135 (1998).

¹¹M. Mezard, G. Parisi, and M.A. Virasoro, *Spin Glass Theory and Beyond* (World Scientific, Singapore, 1987).

¹²K.H. Fischer and J.A. Hertz, *Spin Glasses* (Cambridge University, Cambridge, England, 1991).

¹³R. Pirc, B. Tadić, and R. Blinc, Phys. Rev. B **37**, 679 (1988); T.K. Kopec, B. Tadić, R. Pirc, and R. Blinc, Z. Phys. B: Condens. Matter **78**, 493 (1990).

¹⁴S. Dattagupta, B. Tadić, R. Pirc, and R. Blinc, Phys. Rev. B **44**, 4387 (1991); **47**, 8801 (1993).

¹⁵V. Banerjee and S. Dattagupta, Phase Transitions **62**, 233 (1997).

¹⁶Bog-Gi Kim, Jong-Jean Kim, and Hyun M. Jang, Phys. Rev. B **60**, 7170 (1991).

¹⁷R.V. Chamberlin, R. Böhmer, E. Sanchez, and C.A. Angell, Phys. Rev. B **46**, 5787 (1992).

¹⁸I.A. Akhiezer and A.I. Spol'nik, Fiz. Tverd. Tela (Leningrad) **25**, 148 (1983) [Sov. Phys. Solid State **25**, 81 (1983)].

¹⁹V. Dobrosavljević and R.M. Stratt, Phys. Rev. B **36**, 8484 (1987).

²⁰R. Pirc, B. Tadić, and R. Blinc, Phys. Rev. B **36**, 8607 (1987).

²¹S. Dattagupta, *Relaxation Phenomena in Condensed Matter Physics* (Academic, Orlando, 1987).

²²S.P. Heims, Phys. Rev. **138**, A587 (1965).

²³V. Banerjee and S. Dattagupta, J. Phys.: Condens. Matter **10**, 8351 (1998).

²⁴A. Loidl, R. Fieele, and K. Knorr, Phys. Rev. Lett. **48**, 1263 (1982).

²⁵S. Bhattacharya, S.R. Nagel, L. Fleishman, and S. Susman, Phys. Rev. Lett. **48**, 1267 (1982).

²⁶C.P. Flynn and A.M. Stoneham, Phys. Rev. B **1**, 9366 (1970); Y. Kagan and M.I. Klinger, J. Phys.: Condens. Matter **7**, 2791 (1974).

²⁷For a recent review, see H. Grabert and H. Schrober, in *Hydrogen in Metals III*, Topics in Applied Physics Vol. 73, edited by H. Wipf (Springer-Verlag, Berlin, 1997).